

We are IntechOpen, the world's leading publisher of Open Access books Built by scientists, for scientists

6,900

Open access books available

186,000

International authors and editors

200M

Downloads

Our authors are among the

154

Countries delivered to

TOP 1%

most cited scientists

12.2%

Contributors from top 500 universities



WEB OF SCIENCE™

Selection of our books indexed in the Book Citation Index
in Web of Science™ Core Collection (BKCI)

Interested in publishing with us?
Contact book.department@intechopen.com

Numbers displayed above are based on latest data collected.
For more information visit www.intechopen.com



Collision Detection and Control of Parallel-Structured Flexible Manipulators Based on Unscented Kalman Filter

Yuichi Sawada, Yusuke Watanabe and Junki Kondo

Kyoto Institute of Technology

Department of Mechanical and System Engineering

Japan

1. Introduction

Flexible manipulators that are lightweight and mechanically flexible are useful for operations in various fields, e.g. space development programs, robotic assistants to humans and so forth. However, the derivation of their exact mathematical model and synthesis of the accurate positioning controller is exceptionally difficult because of the mechanical flexibility. On the other hand, the mechanical flexibility is conducive to the safety in collision between the manipulator and the obstacles. However, it is not positive safety measures that reduction of the influence due to the impact force of collision for the flexible manipulator depends only on its mechanical flexibility. In order to develop flexible manipulators so that they work safely with persons cooperatively, we need to introduce the active collision detection and suspension control algorithms to the flexible manipulators.

The functional requirements of safety in the operations of flexible manipulators are as follows: i) to avoid collisions with obstacles placed or moving in the work space; ii) to detect collisions when unlooked-for obstacles contact with the flexible arm of the manipulator and to suspend the motion as immediately as possible; iii) to plan a new path so as to avoid the place of obstacles.

There are several researches on collision detection methods without extra sensors (A. Garcia & Somolinos, 2003), (M. Kaneko & Tsuji, 1998), (T. Matsumoto & Kosuge, 2000). Moorehead and Wang proposed (Moorehead & Wang, 1996) a collision detection method using strain gauges to determine the intensity and position of external force due to collision with a flexible cantilevered beam. The estimation of the contact position in their approach was achieved by the mechanical relation between positions of the two strain gauges and the bending moments measured by the sensors. Payo et al. (I. Payo & Cortazar, 2009) is produced the method of collision detection and suspend control of the very lightweight single-link flexible arm based on coupling torque feedback. They used the variation of the control torque.

The authors have focused our attention on the second item mentioned above. We already developed a method of collision detection for the single-link flexible manipulator using the innovation process of the Kalman filter (Sawada, 2002a), (Sawada, 2002b), (Sawada, 2002c), (Sawada, 2004 (in Japanese)), (Kondo & Sawada, 2008). Our approach requires no particular

sensors for measuring the contact events between the flexible arm and the obstacles. This collision detection method is based on the observation data for vibration control of the flexible manipulator. The mathematical model of the flexible manipulators is expressed by nonlinear partial differential equations and ordinary differential equations, which is regarded as the infinite-dimensional system. The Kalman filter is constructed for the linearized finite-dimensional model corresponding to the mathematical model of the manipulator.

This chapter describes a method of collision detection and suspend control for parallel-structured flexible manipulators subject to random disturbance using unscented Kalman filter (UKF), which is one of the nonlinear filters. The features of the parallel-structured flexible manipulator are that it holds sufficient rigidity along the vertical axis and mechanical flexibility along the displacement axis of the arm (Sawada & Watanabe, 2007). The exact mathematical model of the parallel-structured flexible manipulator is described by quite complex nonlinear partial and ordinary differential equations, because the manipulator consists of two flexible beams which are disposed parallel. In this chapter, the parallel-structured flexible manipulators are approximately modeled by a flexible arm consisting of a flexible beam with the same boundary conditions as the parallel-structured one.

The approximated model of the flexible manipulator is also a nonlinear system. In order to construct the state estimate for the flexible manipulator, we employed the unscented Kalman filter as the nonlinear state estimator (S. Julier & Durrant-Whyte, 2000), (S.J. Julier & Durrant-Whyte, 1997), (Y.-S. Chen & Wakui, 1989). The UKFs are based on the Monte Carlo method, which have been developed by Simon Julier (S. Julier & Durrant-Whyte, 2000), (S.J. Julier & Durrant-Whyte, 1997) in order to improve the accuracy of the extended Kalman filters. The UKF generates a population of so-called sigma-points on the basis of the current mean and covariance of the state vector. The mean and covariance of the state are calculated using these sigma-points, which means that the algorithm is not necessary to evaluate the Jacobians.

Collision between the parallel-structured flexible manipulator and an undesirable obstacle can be detected using the innovation process of the UKF based on the measured data of strain sensors pasted on the side of the manipulator. The UKF is constructed for the nonlinear state space model corresponding to the parallel-structured flexible manipulator without the impact force term due to the collision. The collision detection function is defined by the strength of the innovation process. The detection algorithm decides that the collision occurs if the collision detection function exceeds a preassigned threshold.

The controller for the manipulator has the following two objectives: i) to rotate the flexible arm from the initial position to the desired position; ii) to safely suspend the rotation of the arm when the collision is detected.

2. Mathematical model of parallel-structured single-link flexible manipulator

Consider a parallel-structured single-link flexible arm with collision illustrated in Fig.1. This arm consists of two uniform Euler-Bernoulli beams with their length ℓ . The end of each beam is clamped to an unit of hub and the other end is to a tip-mass.

Let OXY be the inertial Cartesian coordinate system; Oxy the rotating coordinate system around the servomotor shaft at the hub; O_1x_1y and O_2x_2y the rotating coordinate systems for Beam 1 and 2, respectively. $u_i(t, x_i)$ ($i = 1, 2$) denotes the transverse displacement of Beam i from the x_i -axis. Physical parameters of the beams are as follows: ρ the uniform mass

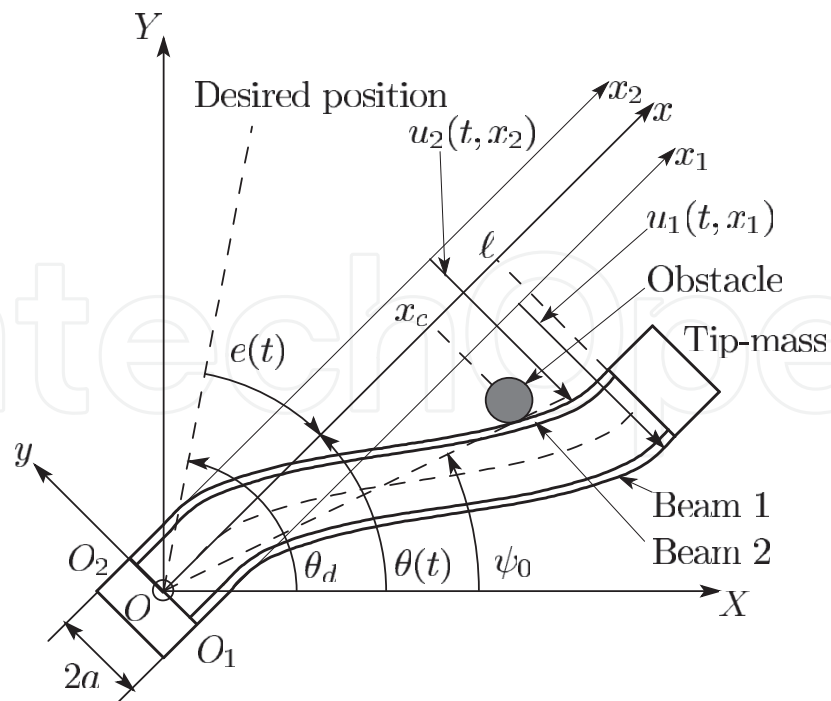


Fig. 1. Parallel-structured single-link flexible arm.

density; S the cross section; EI the uniform flexible rigidity (where E denotes the Young's modulus and I the second moment of cross sectional area); and c_D the coefficient of Kelvin-Voigt type damping. The unit of the hub has the moment of inertia J_0 . The tip-mass has its mass m and the moment of inertia J_1 . It is assumed that the obstacle collides at $x = x_c$ ($0 < x_c < \ell$) at $t = t_c$, where x_c and t_c are all unknown. Ψ_0 denotes the angle of position which is the contact point between the arm and the obstacle, where Ψ_0 is also unknown.

The exact mathematical model of the parallel-structured single-link flexible arm derived by the Hamilton's principle is highly complex. For the sake of simplicity, the parallel-structured single-link flexible arm consisting of two Euler-Bernoulli type beams is approximately modeled by a single-link flexible arm constructed by a flexible beam with the same boundary conditions as the parallel-structured one (see Fig.2). $u(t, x)$ denotes the transverse displacement of the approximated model from the equilibrium state of the beam. $\theta(t)$ is the angle of the tangential axis of the root of the arm from the X -axis; $e(t)$ the error of the rotation angle $\theta(t)$ from the desired position θ_d , i.e. $e(t) := \theta(t) - \theta_d$.

Now we derive the approximated mathematical model of the parallel-structured single-link flexible arm with the collision based on the simple-structured model using the Hamilton's principle. The position vectors of the arbitrary point of the beam, $r(t, x)$, and the mass center of the tip-mass, $p(t)$, are expressed by

$$r(t, x) = \begin{bmatrix} x \cos \theta(t) - \{u(t, x) - a\} \sin \theta(t) \\ x \sin \theta(t) + \{u(t, x) + a\} \sin \theta(t) \end{bmatrix} \quad (1)$$

$$p(t) = \begin{bmatrix} (\ell + h) \cos \theta(t) - u(t, \ell) \sin \theta(t) \\ (\ell + h) \sin \theta(t) + u(t, \ell) \sin \theta(t) \end{bmatrix}, \quad (2)$$

where $2h$ denotes the length of the tip-mass.

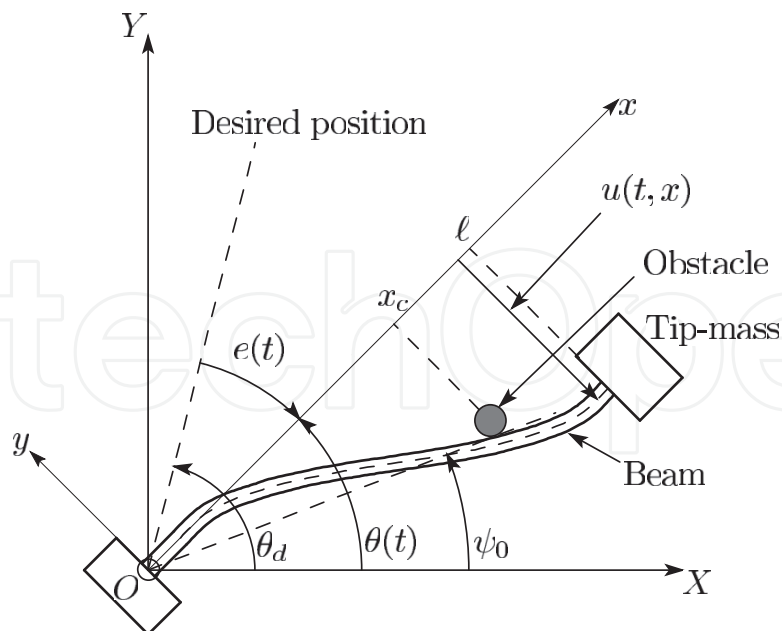


Fig. 2. Simplified structure of parallel-structured single-link flexible arm.

The kinetic energy of rigid part of the arm, $T_R(t)$, is given by the sum of the kinetic energies of the translation motion and rotation of the tip-mass and the rotation of the hub attached to the shaft of the servomotor:

$$T_R(t) = \frac{1}{2}m\|\dot{p}(t)\|^2 + \frac{1}{2}(J_0 + J_1)\dot{\theta}^2(t), \quad (3)$$

where $\|\cdot\|$ denotes the Euclid norm. Similarly, the kinetic energy of the flexible beam is given by

$$T_F(t) = \int_0^{\ell} \hat{T}(t, x) dx, \quad (4)$$

where $\hat{T}(t, x)$ represents the kinetic energy density of flexible part defined by

$$\hat{T}(t, x) := \frac{1}{2} \rho S \|\dot{r}(t, x)\|^2. \quad (5)$$

The total kinetic energy of the arm is expressed by the sum of the kinetic energies of the rigid and flexible parts, i.e.,

$$T(t) = T_R(t) + T_F(t). \quad (6)$$

The potential energy of the whole arm is expressed by

$$V(t) = \int_0^{\ell} \hat{V}(t, x) dx, \quad (7)$$

where $\hat{V}(t, x)$ is the density function of the potential energy of the flexible part given by

$$\hat{V}(t, x) = \frac{1}{2} EI \left\{ \frac{\partial^2 u(t, x)}{\partial x^2} \right\}. \quad (8)$$

The Hamilton's principle is described by the following equation:

$$\int_{t_1}^{t_2} \{ \delta T(t) - \delta V(t) + \delta W_{nc}(t) + s(t)\delta\psi(t) \} dt = 0, \quad (9)$$

where t_1 and t_2 are arbitrary times; $s(t)$ represents the Lagrange multiplier which is equivalent to the external force generated by the collision with the obstacle; and $\delta W_{nc}(t)$ denotes the virtual work due to the nonconservative forces, e.g. internal damping forces of the beams, the control torque and external disturbances. $\psi(t)$ describes the geometric constrained condition between the unlooked-for obstacle and the flexible beam, i.e.

$$\psi(t) = u(t, x_c) - x_c \tan\{\varphi_0 - \theta(t)\} \equiv 0. \quad (10)$$

Let us assume that $|\varphi_0 - \theta(t)|$ is sufficiently small. We can regard $\tan\{\varphi_0 - \theta(t)\} \cong \varphi_0 - \theta(t)$. Then, (10) can be rewritten into

$$\psi(t) = \int_0^\ell u(t, x) \delta(x - x_c) dx - x_c \{\varphi_0 - \theta(t)\} \equiv 0. \quad (11)$$

$\delta W_{nc}(t)$ is expressed by

$$\begin{aligned} \delta W_{nc}(t) = & -\mu\dot{\theta}(t)\delta\theta + \tau(t)\delta\theta + g_\theta\gamma_\theta(t)\delta\theta \\ & - \int_0^\ell c_D \left(\frac{\partial^3 u(t, x)}{\partial x^2 \partial t} \right) \delta u'' dx + \int_0^\ell g_f \gamma(t, x) \delta u dx, \end{aligned} \quad (12)$$

where the prime denotes the differentiation with respect to x ; μ denotes the damping coefficient corresponding to the damping force acting at the shaft of the servomotor; $\tau(t)$ the control torque; $\gamma_\theta(t)$ the random disturbance acting at the rotation of the arm; $\gamma(t, x)$ the distributed random disturbance along the beam due to the aerodynamic resistance; and g_θ and g_f are constants.

As the generalized coordinates, we consider the following variables: $\theta(t)$, $\dot{\theta}(t)$, $u(t, x)$, $\dot{u}(t, x)$, $u'(t, x)$, $u''(t, x)$, $\dot{u}''(t, x)$, $u(t, \ell)$, $\dot{u}(t, \ell)$. Substituting (7), (8) and (11) into (10); in addition, performing a large amount of calculations, we have the following nonlinear differential equations as the mathematical model of the approximated dynamical model corresponding to the parallel-structured single-link flexible manipulator:

$$\begin{aligned} \rho S \frac{\partial^2 u(t, x)}{\partial t^2} + c_D I \frac{\partial^5 u(t, x)}{\partial x^4 \partial t} + EI \frac{\partial^4 u(t, x)}{\partial x^4} = & -\rho S x \ddot{\theta}(t) + \rho S \dot{\theta}^2(t) u(t, x) + g_1 \gamma(t, x) \\ & + s(t) \delta(x - x_c) - \left\{ m(\ell + h) \ddot{\theta}(t) + m \frac{\partial^2 u(t, x)}{\partial t^2} - m \dot{\theta}^2(t) u(t, x) \right\} \delta(x - \ell), \end{aligned} \quad (13)$$

where $\gamma(t, x)$ the distributed random disturbance modeled by the white Gaussian noise; g_1 and h are constants; $\delta(\cdot)$ denotes the Dirac's delta function; and $s(t)$ the magnitude of collision input. Assuming that the collision occurs momentarily, the magnitude of collision is assumed to be expressed by $s(t) := s_0 \delta(t - t_c)$, where s_0 and t_c are all unknown. The initial and boundary conditions of (13) are

$$I.C.: u(0, x) = \frac{\partial u(0, x)}{\partial t} = 0 \quad (14)$$

$$B.C.: u(t, 0) = \frac{\partial u(t, 0)}{\partial x} = \frac{\partial u(t, \ell)}{\partial x} = \frac{\partial^3 u(t, \ell)}{\partial x^3} = 0. \quad (15)$$

The initial condition of the error of rotation $e(t)$ is given by $e(0) = \theta_0 - \theta_i$, where θ_0 is initial angle position of the arm.

The dynamics of rotation is given by the following nonlinear differential equation:

$$\begin{aligned} & \left[J_0 + J_1 + mu^2(t, \ell) + mh(\ell + h) + \rho S \int_0^\ell u^2(t, x) dx \right] \ddot{e}(t) \\ & + \left[\mu_\theta + 2mu(t, \ell)\dot{u}(t, \ell) + \rho S \int_0^\ell 2u(t, x)\dot{u}(t, x) dx \right] \dot{e}(t) + mh\ddot{u}(t, \ell) \\ & - \left[\rho S \int_0^\ell u(t, x) dx - m\ell u(t, \ell) \right] \dot{e}^2(t) - \int_0^\ell x \left[c_D I \frac{\partial^5 u(t, x)}{\partial x^4 \partial t} + EI \frac{\partial^4 u(t, x)}{\partial x^4} \right] dx \\ & + \int_0^\ell g_1 x \gamma(t, x) dx - \tau(t) - g_\theta \gamma_\theta(t) = 0. \end{aligned} \quad (16)$$

The observation data is obtained by means of P strain sensors pasted at $x = \xi_j$, ($j = 1, \dots, P$) and a potentiometer installed at the shaft of the hub, i.e.

$$y_0(t) = c_0 e(t) + e_0 \beta_0(t) \quad (17)$$

$$y_j(t) = c_j \int_{\xi_j}^{\xi_j + b_s} \frac{\partial^2 u(t, x)}{\partial x^2} dx + e_j \beta_j(t), \quad (18)$$

where c_j and e_j are constants; and $\beta_j(t)$, ($j = 0, 1, \dots, P$) represents the observation noise which is modeled by the white Gaussian noise. In order to use the finite-dimensional controller and state estimator, the dynamics of the arm described by (13) and (16) are converted into the stochastic finite-dimensional state space model via the modal expansion technique,

$$u(t, x) = \sum_{k=1}^N u_k(t) \phi_k(x), \quad (19)$$

where $\{u_k(t)\}_{k=1, \dots, N}$ denote the modal displacements; N the large positive number; $\phi_k(x)$ the eigenfunction (mode function) of the following eigenvalue problem with respect to the operator $\mathcal{A} = \{(EI)/(\rho S)\}(d^4/dx^4)$:

$$\mathcal{A}\phi_k(x) = \lambda_k \phi_k(x). \quad (20)$$

Introducing the state vector defined by $v(t) = [u_1(t), \dots, u_N(t), \dot{u}_1(t), \dots, \dot{u}_N(t), e(t), \dot{e}(t)]^T$, the state space model of the approximated flexible arm can be described by the following stochastic differential equation:

$$\dot{v}(t) = A(v)v(t) + b(v)\tau(t) + G(v)\gamma(t) + g_c(v; x_c)s(t) \quad (21)$$

$$y(t) = Cv(t) + E\beta(t), \quad (22)$$

where $\gamma(t) = [\gamma_1(t), \dots, \gamma_N(t), \gamma_\theta(t)]^T$; $\gamma_k(t) = \int_0^\ell \gamma(t, x)\phi_k(x)dx$; $\beta(t) := [\beta_0(t), \beta_1(t), \dots, \beta_p(t)]^T$; $\mathcal{E}\{\gamma(t)\gamma^T(\tau)g\} = W\delta(t - \tau)$; $\mathcal{E}\{\beta(t)\beta^T(\tau)\} = V\delta(t - \tau)$ ($\mathcal{E}\{\cdot\}$: mathematical expectation).

3. Nonlinear state estimation using UKF

The state space model described by (21) and (22) is a stochastic nonlinear system with the collision input. In order to control the tip position and to reduce the random vibration of the whole flexible manipulator, the information of the state $v(t)$ is required. However, the collision input affects as an unknown disturbance. For achieving these purposes, the unscented Kalman filter (UKF) for the following collision-free system is employed:

$$\dot{v}_f(t) = A(v_f)v_f(t) + B(v_f)f(t) + G(v_f)\gamma(t), \quad (23)$$

where $v_f(t)$ denotes the state vector of collision-free system.

The UKF is constructed for the discrete-time nonlinear stochastic system given by equation (23) that is the continuous-time system. Equation (23) and (22) can be converted into the discretized version of the system. By using the Runge-Kutta method, (22) and (23) are rewritten into the following nonlinear discrete-time system:

$$v_f(k+1) = F(v_f(k), \tau(k), \gamma(k)) \quad (24)$$

$$y(k) = Cv(k) + E\beta(k), \quad (25)$$

where k denotes the time-step; Δt the time interval; and $F(\cdot)$ the nonlinear function defined by

$$F(v_f(k), \tau(k), \gamma(k)) = v_f(k) + \frac{\Delta t}{6} \{H_1(v_f(k), \tau(k), \gamma(k)) + 2H_2(v_f(k), \tau(k), \gamma(k)) + 2H_3(v_f(k), \tau(k), \gamma(k)) + H_4(v_f(k), \tau(k), \gamma(k))\} \quad (26)$$

$$H_1(v_f(k), \tau(k), \gamma(k)) = A(v_f(k))v_f(k) + B(v_f(k))\tau(k) + G(v_f(k))\gamma(k)$$

$$H_2(v_f(k), \tau(k), \gamma(k)) = A(v_f(k))\{v_f(k) + H_1(\cdot)\Delta t / 2\} + B(v_f(k))\tau(k) + G(v_f(k))\gamma(k)$$

$$H_3(v_f(k), \tau(k), \gamma(k)) = A(v_f(k))\{v_f(k) + H_2(\cdot)\Delta t / 2\} + B(v_f(k))\tau(k) + G(v_f(k))\gamma(k)$$

$$H_4(v_f(k), \tau(k), \gamma(k)) = A(v_f(k))\{v_f(k) + H_3(\cdot)\Delta t\} + B(v_f(k))\tau(k) + G(v_f(k))\gamma(k).$$

The algorithm of UKF is summarized the three steps as follows:

Step 1. The $(2N + 2)$ -dimensional random variable $v_f(k)$ is approximated by $2(2N + 2) + 1$ sigma points \mathcal{X}_i with weight coefficients W_i .

$$\mathcal{X}_0 = \hat{v}_f(k | k) \quad (27)$$

$$W_0 = \frac{\kappa}{2N + 2 + \kappa} \quad (28)$$

$$\mathcal{X}_i = \hat{v}_f(k|k) + \{\sqrt{(2N+2+\kappa)P(k|k)}\}_i \quad (29)$$

$$W_i = \frac{1}{2(2N+2+\kappa)} \quad (30)$$

$$\mathcal{X}_{i+2N+2} = \hat{v}_f(k|k) - \{\sqrt{(2N+2+\kappa)P(k|k)}\}_i \quad (31)$$

$$W_{i+2N+2} = \frac{1}{2(2N+2+\kappa)}, \quad (i = 1, \dots, 2N+2) \quad (32)$$

where κ denotes the integer scaling parameter; W_i the weight coefficient that is associated with the i -th point and $\{\sqrt{(2N+2+\kappa)P(k|k)}\}_i$ represents the i -th column of the matrix U satisfying $M = UU^T$ if $M := (2N+2+\kappa)P(k|k)$. In this paper, the matrix U is calculated via the incomplete Cholesky decomposition (Saad, 1996).

Step 2. Transform each point through the nonlinear function $F(\cdot)$, and the predicted mean, covariance and observation, the innovation covariance $P_{yy}(k+1|k)$ and the cross correlation matrix $P_{xy}(k+1|k)$ are computed as follows:

$$\mathcal{X}_i(k+1|k) = F(\mathcal{X}_i(k|k), \tau(k), 0) \quad (33)$$

$$\hat{v}_f(k+1|k) = \sum_{i=0}^{2(2N+2)} W_i \mathcal{X}_i(k+1|k) \quad (34)$$

$$P(k+1|k) = \sum_{i=0}^{2(2N+2)} W_i \{\mathcal{X}_i(k+1|k) - \hat{v}_f(k+1|k)\} \\ \times \{\mathcal{X}_i(k+1|k) - \hat{v}_f(k+1|k)\}^T + GWG^T \quad (35)$$

$$\mathcal{Y}_i(k+1|k) = C\mathcal{X}_i(k+1|k) \quad (36)$$

$$\hat{y}_i(k+1|k) = \sum_{i=0}^{2(2N+2)} W_i \mathcal{Y}_i(k+1|k) \quad (37)$$

$$P_{yy}(k+1|k) = \sum_{i=0}^{2(2N+2)} W_i \{\mathcal{Y}_i(k+1|k) - \hat{y}_i(k+1|k)\} \\ \times \{\mathcal{Y}_i(k+1|k) - \hat{y}_i(k+1|k)\}^T + EVE^T \quad (38)$$

$$P_{vy}(k+1|k) = \sum_{i=0}^{2(2N+2)} W_i \{\mathcal{X}_i(k+1|k) - \hat{v}_f(k+1|k)\} \\ \times \{\mathcal{Y}_i(k+1|k) - \hat{y}_i(k+1|k)\}^T. \quad (39)$$

Step 3. The state estimate and covariance are given through updating the prediction by the linear update rule which is specified by the weights chosen to minimize the mean squared error of the estimate. The update rule is

$$\hat{v}_f(k+1|k+1) = \hat{v}_f(k+1|k) + K(k+1)\{y(k+1) - \hat{y}(k+1|k)\} \quad (40)$$

$$P(k+1|k+1) = P(k+1|k) - K(k+1)P_{yy}(k+1|k)K^T(k+1|k), \quad (41)$$

where $K(k+1)$ is the Kalman filter gain given by

$$K(k+1) = P_{vy}(k+1|k)P_{yy}^{-1}(k+1|k). \quad (42)$$

4. Collision detection algorithm

It is an undesirable accident that the flexible manipulator collides with an unknown obstacle, because the collision input $s(t)$ affects the state of flexible manipulators as the disturbance. The problem of the collision detection is considered as a detection problem of the abrupt change from the collision-free system to the system with the collision. The change of the systems can be detected using the observation data measured by the piezoelectric sensors pasted at the root of the flexible arm. In other words, the collision is detected by making a decision whether the observation data $y(t)$ is provided from the collision included model or the collision-free model.

For this purpose, the intensity of the innovation process is used. The innovation process of the UKF, $\mu(k)$, is defined by the difference between the actual observation data and the estimated observation data measuring collision-free system, i.e.,

$$\mu(k) = y(k) - C\hat{v}_f(k|k), \quad (43)$$

where $\hat{v}_f(k|k)$ is the estimate of $v_f(k)$ which is calculated by the UKF mentioned in the previous Section. Substituting (25) into (43), we have

$$\mu(k) = Cz(k) + E\beta(k), \quad (44)$$

where $z(k)$ is the estimation error defined by $z(k) := v(k) - \hat{v}_f(k|k)$. If the collision does not occur, the state vector $v(k)$ is equal to $v_f(k)$. However, if the collision occurs, $v(k)$ is equal to the state vector of collision model. In this case, $z(k)$ becomes large because of the collision input. In order to detect the collision, the following scalar function (*collision detection function*) is introduced:

$$r(k) = \mu^T(k)\mu(k). \quad (45)$$

If the collision detection function $r(k)$ exceeds a threshold ε , then the collision has occurred. In fact, it is assumed that the estimation error when the collision has occurred is separated as

$$z(k) = \tilde{z}(k) + \alpha(k), \quad (46)$$

where $\tilde{z}(k)$ is the estimation error of the UKF based on the collision-free system; and $\alpha(k)$ the estimation error caused by the collision input. Substituting (46) into (44), the innovation process $\mu(k)$ is rewritten into

$$\mu(k) = C\tilde{z}(k) + C\alpha(k) + E\beta(k). \quad (47)$$

From equations (45) and (47), the mathematical expectation of the collision detection function $r(k)$ is evaluated by

$$\mathcal{E}\{r(k)\} = \text{tr}\{CP_z(k)C^T\} + \text{tr}\{EVE^T\} + \text{tr}\{C\alpha^T(k)\alpha(k)C^T\}, \quad (48)$$

where $P_z(k) := \mathcal{E}\{\tilde{z}^T(k)\tilde{z}(k)\}$. The first two terms in the right-hand side of (48) is the bias depending on the observation and the system noises. The third term is caused by the collision input which is the deterministic process. If the third term becomes sufficiently large, then $r(k)$ becomes also large at the time when the collision occurs.

5. Position and suspend control

The purpose of controller is to generate the control torque for the servomotor so that the tip position of the flexible manipulator follows the reference trajectory. In this work, the sliding mode controller is employed (Utkin, 1992). The flexible manipulator is controlled so that its state converges to the equilibrium state.

The sliding mode controller is constructed for the following deterministic collision-free system:

$$\dot{v}_f(t) = A(v_f(t))v_f(t) + B(v_f(t))\tau(t) \quad (49)$$

which has no system noise term. If the flexible manipulator is well controlled, the error state vector $v_f(t)$ is assumed to sufficiently be small, i.e. $\|v_f(t)\| \ll 1$. In this work, we consider that the matrices $A(v_f(t))$ and $B(v_f(t))$ can be approximated as $A(v_f(t)) \cong A(0)$ and $B(v_f(t)) \cong B(0)$. Using these approximations, the error system is rewritten into the following equation:

$$\dot{v}_f(t) = A_e v_f(t) + B_e \tau(t), \quad (50)$$

where A_e and B_e are constant matrices defined by

$$A_e := A(0), \quad B_e := B(0). \quad (51)$$

The objectives of the sliding mode controller are to control the tip position, to suppress the random vibration of the whole manipulator, and to suspend the motion of the manipulator when a collision is detected. The control torque $\tau(t)$ is generated by the sliding mode controller. The output of the controller can be separated into two parts, i.e.:

$$\tau(t) = f_{eq}(t) + f_{nl}(t), \quad (52)$$

where $f_{eq}(t)$ represents the term of linear control input called the equivalent control input in the sliding mode; and $f_{nl}(t)$ the term of nonlinear control input in the reaching mode.

The switching function $\sigma(t)$ is given by

$$\sigma(t) = Sv_f(t), \quad (53)$$

where S represents the gradient of the switching plane. In the sliding mode, the switching function $\sigma(t)$ holds the following conditions:

$$\sigma(t) = 0 \quad (54)$$

$$\dot{\sigma}(t) = 0. \quad (55)$$

The equivalent control input is obtained using (50), (53) and (55) as:

$$f_{eq}(t) = -(SB_e)^{-1}SA_e v_f(t). \quad (56)$$

Substituting (56) into (50), the equivalent control system can be described by

$$\dot{v}_f(t) = \{A_e - B_e(SB_e)^{-1}SA_e\}v_f(t) \equiv \tilde{A}_e v_f(t), \quad (57)$$

where $\tilde{A}_e := A_e - B_e(SB_e)^{-1}SA_e$.

In order to find the switching plane, we consider the cost functional defined by

$$J = \int_0^t \left\{ \int_0^\ell [q_1 \{\dot{u}(s,x)\}^2 + q_2 \{u(s,x)\}^2 + q_3 \{\ddot{u}(s,x)\}^2 + q_4 \{u''(s,x)\}^2] dx + q_5 \dot{e}^2(s) + q_6 e^2(s) \right\} ds, \quad (58)$$

where q_i ($i = 1, \dots, 6$) are positive constants. Substituting the solution of the system described by the equation (13) given by (19) into this, it is rewritten into the following expression:

$$J = \int_0^T v_f^T(t) Q v_f(t) dt, \quad (59)$$

where $Q := \text{diag}\{\Theta_1, \Theta_2, q_5, q_6\}$; $\Theta_1 = q_1 I_N + q_3 \Psi$; $\Theta_2 = q_2 I_N + q_4 \Psi$; (I_N : N -dimensional unit matrix); and

$$\Psi = \begin{bmatrix} \int_0^\ell \phi_1''(x)\phi_1''(x)dx & \dots & \int_0^\ell \phi_1''(x)\phi_N''(x)dx \\ \vdots & & \vdots \\ \int_0^{\ell_i} \phi_N''(x)\phi_1''(x)dx & \dots & \int_0^\ell \phi_N''(x)\phi_N''(x)dx \end{bmatrix}. \quad (60)$$

The gradient of the switching plane S must be decided so that the eigenvalues of \tilde{A}_e becomes stable. There are a method to choose S as a feedback gain of the optimal control. Namely, S is determined as follows (Y.-S. Chen & Wakui (1989)):

$$S = B_e^T P \quad (61)$$

$$PA_e + A_e^T P - PB_e B_e^T P + Q = 0. \quad (62)$$

The nonlinear control input in reaching mode is considered. The sliding mode control is regarded as variable structure control as a required condition. So, using the switching function $\sigma(t)$, the term of nonlinear control input $f_{nl}(t)$ is defined by

$$f_{nl}(t) = -F \text{sgn}(\sigma(t)), \quad (63)$$

where F is the nonlinear controller gain; and $\text{sgn}(\cdot)$ the signum function. Therefore, the control input $f(t)$ is given by

$$\tau(t) = -(SB_e)^{-1} SA_e v_f(t) - F \operatorname{sgn}(\sigma(t)). \quad (64)$$

In order to achieve $\sigma(t) \rightarrow 0$ ($t \rightarrow \infty$), the Lyapunov function for the switching function is chosen as

$$V(t) = \frac{1}{2} \sigma^T(t) \sigma(t). \quad (65)$$

The time derivative of the the Lyapunov function defined by (65) is described with (50) and (64) by

$$\dot{V}(t) = -\sigma^T(t) SB_e F \operatorname{sgn}(\sigma(t)). \quad (66)$$

If $\dot{V}(t) < 0$, the switching function converges to zero. Hence, the nonlinear control gain F must satisfy the following condition:

$$F \begin{cases} > 0 & : \text{if } SB_e > 0 \\ < 0 & : \text{if } SB_e < 0. \end{cases} \quad (67)$$

At the neighborhood of the switching plane, the signum function raises the chattering. So, the signum function is approximated as follows:

$$\operatorname{sgn}(\sigma(t)) = \frac{\sigma(t)}{\|\sigma(t)\|} \approx \frac{\sigma(t)}{\|\sigma(t)\| + \delta}, \quad (68)$$

where δ is a positive constant. As a result, (64) is rewritten into

$$\tau(t) = -(SB_e)^{-1} SA_e v_f(t) - F \frac{\sigma(t)}{\|\sigma(t)\| + \delta}. \quad (69)$$

Because of using the unscented Kalman filter, it is necessary that the switching function $\sigma(t)$ and the controller input $\tau(t)$ given by the sliding mode controller with the UKF are converted into the discretized version given by

$$\sigma(k) = S \hat{v}_f(k) \quad (70)$$

$$\tau(k) = -(SB_e)^{-1} SA_e \hat{v}_f(k) - F \frac{\sigma(k)}{\|\sigma(k)\| + \delta}. \quad (71)$$

When the collision occurs, it is necessary that the flexible manipulator is suspended because of absorbing the impact of collision. The proposed flexible manipulator is controlled by tracking the reference trajectory using the sliding mode controller. For suspending the motion of the manipulator, we consider that the reference trajectory (position control) is changed into a steady position when the collision occurs. The angle position of flexible manipulator at the time t_c when the collision occurs is given by

$$\theta(t_c) = \theta_c, \quad (72)$$

After the collision occurred, the reference trajectory is changed into the trajectory given by the following equation:

$$\theta_d(t) \equiv \theta_c. \quad (73)$$

The desired position becomes the position that the flexible manipulator collides with the obstacle. Then, the flexible manipulator can be suspended at this position.

6. Simulation studies

In this section, several numerical results are presented. The flexible beam is assumed to be made with the phosphor bronze. The physical parameters and the coefficients of the flexible manipulator are listed in Table 1. The observation data is supposed to be measured by piezoelectric sensors with their length $b_s = 3 \times 10^{-2}$ [m] and width 1.2×10^{-2} [m] pasted at $\xi_1 = 3 \times 10^{-3}$ [m] and potentiometers installed at each hub. The parameters of the observation system were set as $c_0 = 10$, $c_1 = 1$, $e_0 = e_1 = 1$. The parameter for the UKF κ was set as $\kappa = 1$. The covariance matrices for the system and observation noises were given by $W = 10^{-5} \times I_{2N+2}$, $V = 10^{-8} \times I_2$. The number of modes of the system was set as $N = 2$. The time partition in numerical simulation was set as $\Delta t = 1 \times 10^{-3}$ [s].

The initial condition of state vector were set as $u(0, x) = 0$ [m], $\dot{u}(0, x) = 0$ [m/s], $\dot{\theta}(0) = 0$ [rad/s] and $\theta(0) = 0$ [rad]. The initial condition of the state vector of the control error system was also set as zero. The weight coefficients of cost functional for the hyperplane S were set as the values; $q_1 = 100$, $q_2 = 100$, $q_3 = 100$, $q_4 = 5$, $q_5 = 4500$, $q_6 = 200$. The nonlinear controller gain was $F = 4$, $\delta = 10$ and the simulation study was carried out for 5 seconds.

Parameters	Values
l_1	0.3[m]
E	1.1×10^5 [MPa]
S	2×10^{-5} [m ²]
ρ	8.8×10^3 [kg/m ²]
c_D	4.84×10^7 [N·s/m ²]
J_0	5 [kg·m ²]
J_1	0.08 [kg·m ²]
m	0.61 [kg]
h	0.026 [m]
g_1	0.05
g_2	0.4

Table 1. Physical parameters of the flexible manipulator.

6.1 Position control

The simulation results of the position control in the collision-free case are shown in Figs.3-6. Fig.3 depicts the angle $\theta(t)$ and its estimate computed by the UKF $\hat{\theta}(t)$. The estimation error with respect to $\theta(t)$ sufficiently small. The controlled angle has converged at the desired position using the UKF based sliding mode control. Figs. 4 and 5 presents the observation

data of the strain measured by the piezoelectric sensor $y_1(t)$ and the displacement of the tip mass $u(t, \ell)$, respectively. Furthermore, Fig.5 also depicts the estimate of the tip-mass displacement $\hat{u}(t, \ell)$ which is calculated by $\hat{u}(t, \ell) = \sum_{i=1}^N \hat{u}_i(t) \phi_i(\ell)$. The estimation error of the tip-displacement based on the noisy observation data (see Figure 4) is adequately small for suppressing the vibration of the tip-mass. Fig.6 shows the response of the control torque $\tau(t)$.

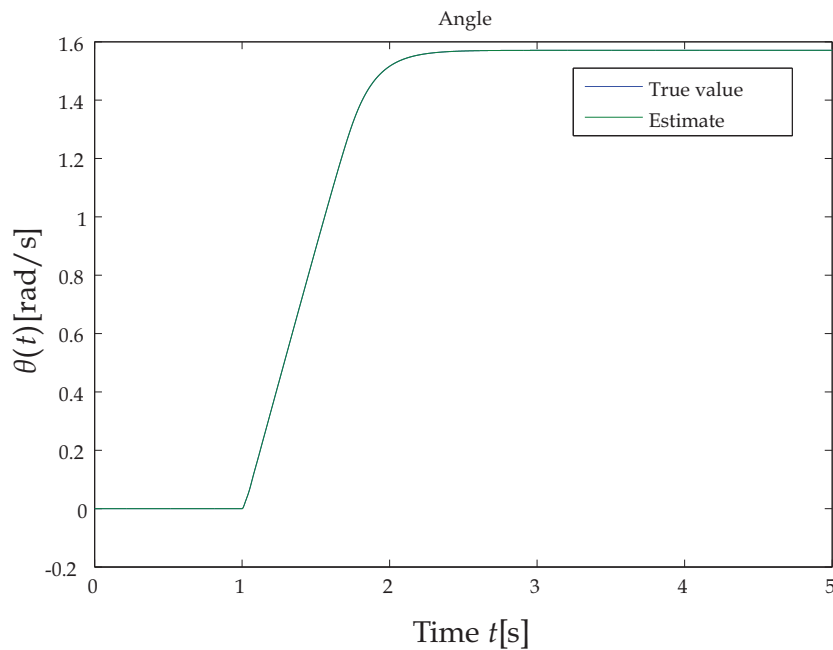


Fig. 3. Behavior of the rotational angle $\theta(t)$ and its estimate $\hat{\theta}(t)$ obtained using the UKF in the collision-free case. The solid line and the dashed line depict the true state of the angle $\theta(t)$ and its estimate $\hat{\theta}(t)$, respectively

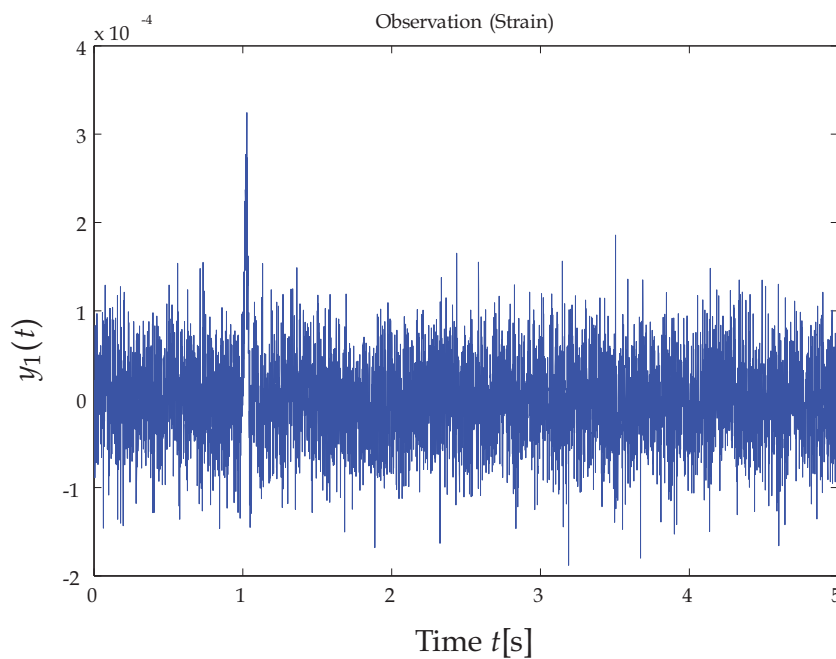


Fig. 4. Observation data of the strain measured by the piezoelectric sensor, $y_1(t)$ in the collision-free case.

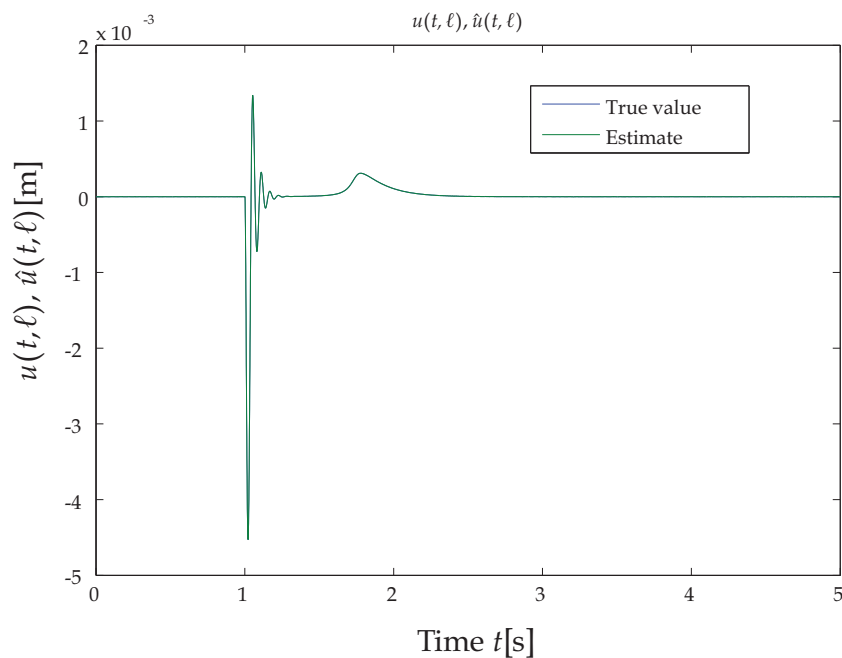


Fig. 5. Displacement of the tip mass $u(t, \ell)$ and its estimate $\hat{u}(t, \ell)$.

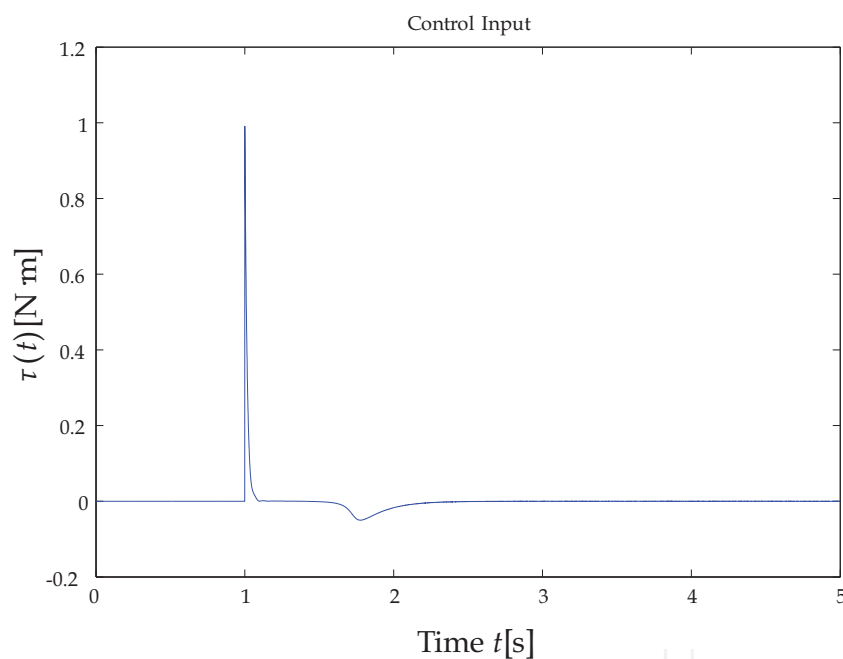


Fig. 6. Control torque $\tau(t)$ generated by the sliding mode controller in the collision-free case.

6.2 Collision detection and suspend control

The simulation results in the collision case are shown in Figs.7-11. In this case, the desired position θ_d was set as the same as in the collision-free case. Figure 7 shows the behavior of the collision detection function given by equation (45). We considered that the collision between the parallel-structured single-link flexible manipulator and the unlooked-for obstacle occurs at $t_c = 1.24[s]$. The value of $r(t)$ before the collision occurs is very small. When the collision occurs at $t = t_c$, the value of $r(t)$ abruptly increases. As seen in Fig. 8, the

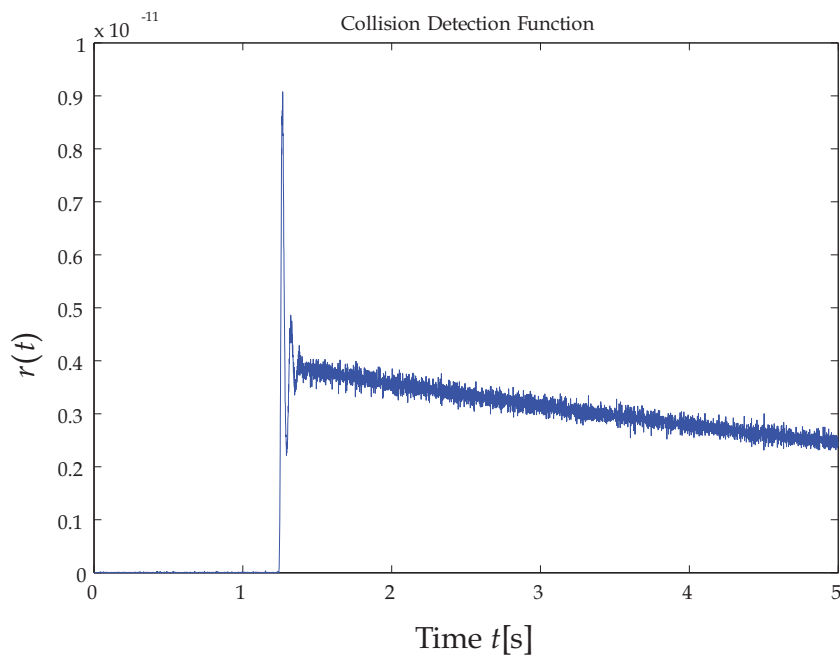


Fig. 7. Behavior of the collision detection function $r(t)$ generated by the innovation process of the UKF in the collision case. The collision occurs at $t_c = 1.24$ [s].

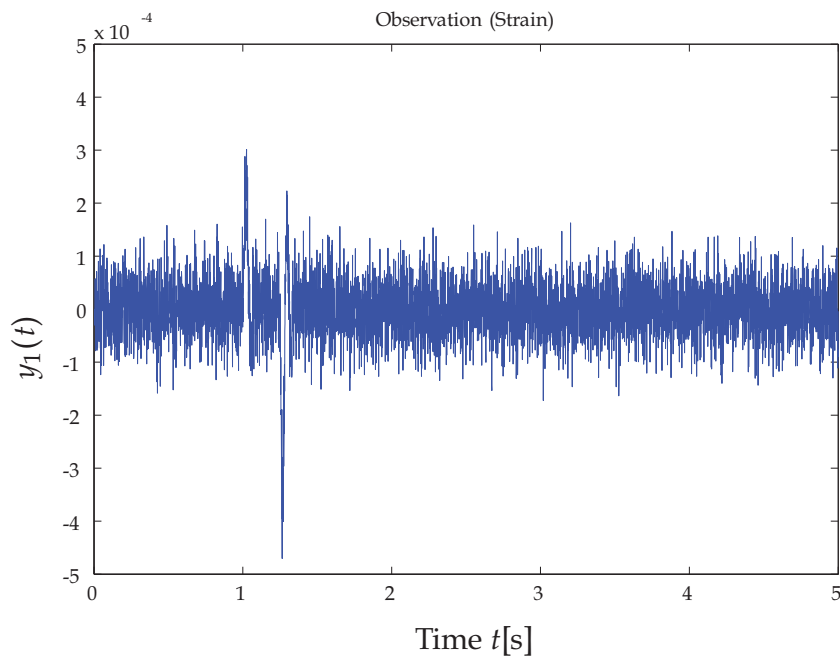


Fig. 8. Observation data of the strain measured by the piezoelectric sensor, $y_1(t)$ in the collision case.

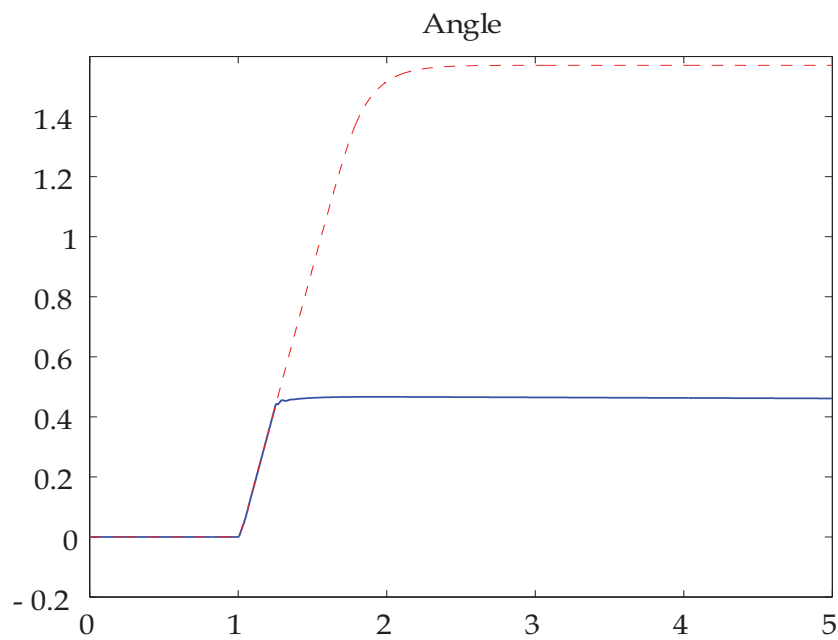


Fig. 9. Behavior of the rotational angle $\theta(t)$ obtained using the UKF in the collision-free and the collision cases. The solid line and the dashed line depict the angle $\theta(t)$ in the collision and collision-free cases, respectively.

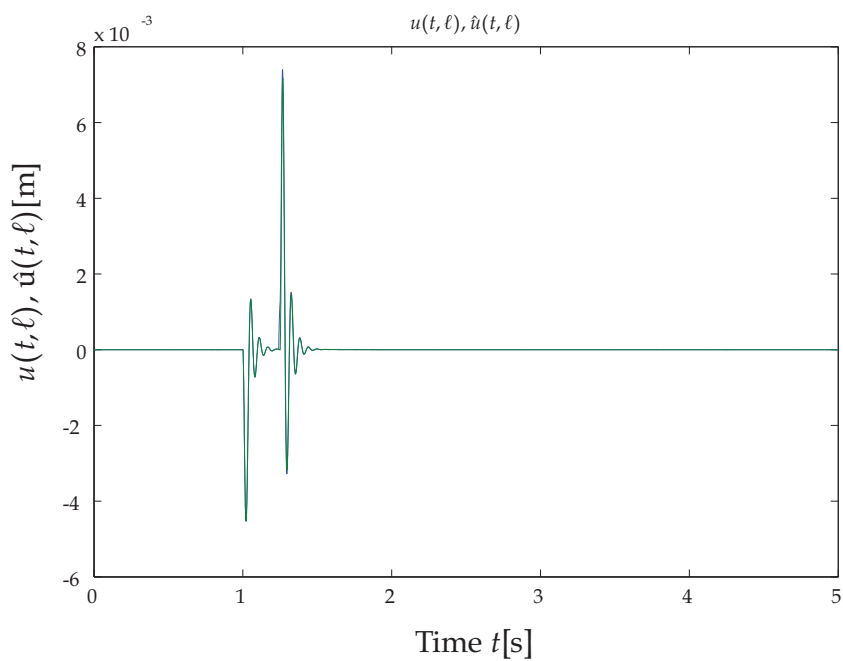


Fig. 10. Displacement of the tip mass $u(t, \ell)$ and its estimate $\hat{u}(t, \ell)$.

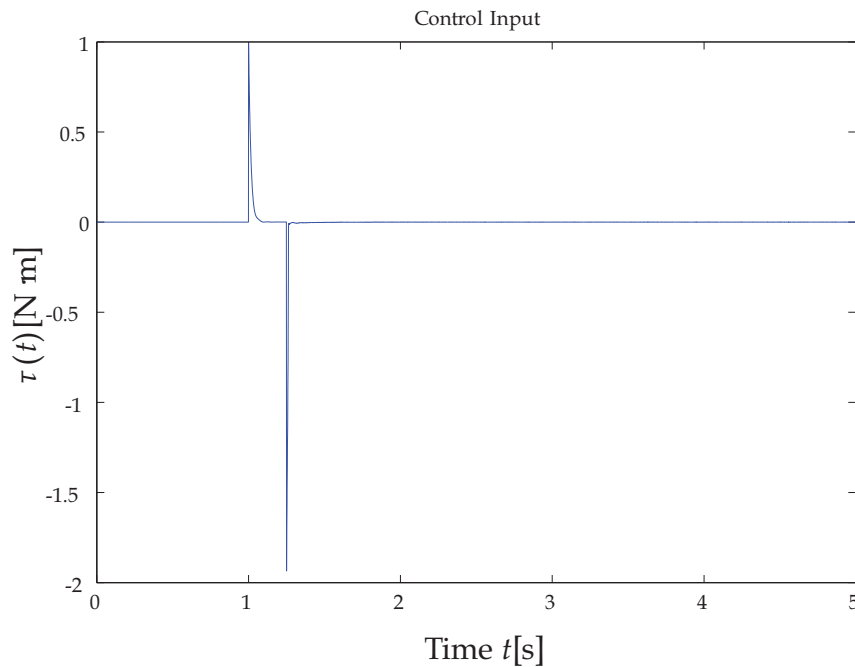


Fig. 11. Control torque $\tau(t)$ generated by the sliding mode controller in the collision case.

observation data of the strain is very noisy. From Figs. 7 and 8, we can see that the collision detection function can detect the weak collision based on the noisy observation data.

The results of the suspend control are shown in Figs. 9 and 10. The rotation of the manipulator was interrupted when the collision has been detected using the collision detection function (see Figure 9). After $r(t)$ exceeded the preassigned threshold $\varepsilon = 1 \times 10^{-12}$, the desired position has been changed from θ_d to $\theta(t_c)$. The displacement of the tip-mass $u(t, \ell)$ shows the vibration with large amplitude after the collision was detected (Fig. 10). The control torque is depicted in Fig. 11. This figure explains that the control torque when the motion of the manipulator was suspended requires the torque of large value.

7. Conclusions

This chapter has presented the new collision detection method and the suspend control of parallel-structured single-link flexible manipulators using the unscented Kalman filter and the sliding mode control. The main result is that the collision detection was achieved using the innovation process of the UKF which is one of the nonlinear filters. Furthermore, the high performance suspend control has been constructed using the sliding mode controller based on the UKF. The proposed approach brings an advantage that the system model requires no linearization. In our previous work, the linearized mathematical model was required because of using the Kalman filter and the LQG controller for collision detection

and control. The proposed collision detection method can be applied to the multi-link flexible manipulators, which have strong nonlinearity.

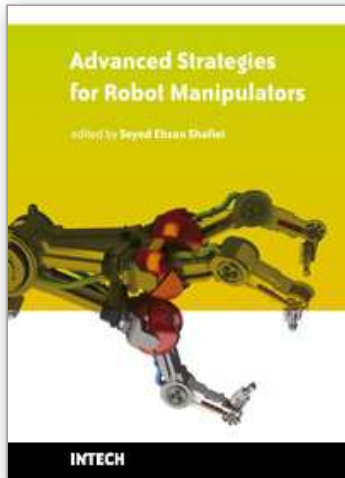
8. References

- García, A.; Feliu, V. & Somolions, J. A. (2003). Experimental testing of a gauge based collision detection mechanism for a new three-degree-of-freedom flexible robot, *Journal of Robotics Systems* Vol. 20(No. 6): 271–284.
- Payo, I.; Feiu V. & Cortazar, O. D. (2009). Force control of very lightweight single-link flexible arm based on coupling torque feedback, *Mechatronics* Vol. 19: 334–337.
- Kondo, J. & Sawada, Y. (2008). Collision detection and suspend control of parallel-structured single-link flexible arms, *Proceedings of SICE Annual Conference 2008, Tokyo* pp. 3250–3255.
- Kaneko, M.; Kanayama, N. & Tsuji, T. (1998). Active antenna for contact sensing, *IEEE Transactions on Robotics and Automation* Vol. 14(No. 2): 278–291.
- Moorehead, S. & Wang, D. (1996). Active antenna for contact sensing, *Proceedings of IEEE International Conference on Robotics and Automation* pp. 804–809.
- Julier, S.; Uhlmann, J. & Durrant-Whyte, H. F. (2000). A new method for the nonlinear transformation of means and covariances in filters and estimators, *Transaction on Automatic Control* Vol. 45(No. 3): 477–482.
- Saad, Y. (1996). *Iterative Methods for Sparse Linear Systems*, PWS Publishing Company.
- Sawada, Y. (2002a). Collision detection for a flexible cantilever-beam subject to random disturbance based on innovation process, *Proceedins of IEEE International Conference on Control Applications* pp. 1171–1176.
- Sawada, Y. (2002b). Collision estimation for a flexible cantilevered-beam subject to random disturbance, *Proceedins of 34th ISCIE Int. Symp. on Stochastic Systems Theory and Its Application* pp. 183–188.
- Sawada, Y. (2002c). Detection of collisions for a flexible beam subject to random disturbance, *Proceedins of 41st SICE Annual Conference* pp. 268–273.
- Sawada, Y. (2004 (in Japanese)). On-line collision detection for flexible cantilevered beams using innovation process, *Transaction of The Institute of Systems, Control and Information Engineers* pp. 349–357.
- Sawada, Y. & Watanabe, T. (2007). Lqg control of a parallel-structured single-link flexible arm, *Proceedings of 51st Annual Conference of ISCIE* pp. 372–373.
- Julier, S.; Uhlmann, J. & Durrant-Whyte, H. F. (1997). A new extension of the kalman filter to nonlinear systems, *Proceedings of AeroSense: 11th International Symposium Aerospace/Defense Sensing, Simulation Control*.
- Matsumoto, T. & Kosuge, K. (2000). Collision detection of manipulator based on adaptive control law, *Proceedings of 2001 IEEE/ASME International Conference on Advanced Intelligent Mechanics* pp. 177–182.
- Utkin, V. I. (1992). *Sliding modes in optimization and control problems*, Springer, New York.

Chen, Y.-S.; Ikeda, H.; Mita, T. & Wakui, S. (1989). Trajectory control of robot arm using sliding mode control and experimented results, *Journal of the Robotics Society of Japan* Vol. 7(No. 6): 706-711.

IntechOpen

IntechOpen



Advanced Strategies for Robot Manipulators

Edited by S. Ehsan Shafiei

ISBN 978-953-307-099-5

Hard cover, 428 pages

Publisher Sciyo

Published online 12, August, 2010

Published in print edition August, 2010

Amongst the robotic systems, robot manipulators have proven themselves to be of increasing importance and are widely adopted to substitute for human in repetitive and/or hazardous tasks. Modern manipulators are designed complicatedly and need to do more precise, crucial and critical tasks. So, the simple traditional control methods cannot be efficient, and advanced control strategies with considering special constraints are needed to establish. In spite of the fact that groundbreaking researches have been carried out in this realm until now, there are still many novel aspects which have to be explored.

How to reference

In order to correctly reference this scholarly work, feel free to copy and paste the following:

Yuichi Sawada, Yusuke Watanabe and Junki Kondo (2010). Collision Detection and Control of Parallel-Structured Flexible Manipulators Based on Unscented Kalman Filter, *Advanced Strategies for Robot Manipulators*, S. Ehsan Shafiei (Ed.), ISBN: 978-953-307-099-5, InTech, Available from: <http://www.intechopen.com/books/advanced-strategies-for-robot-manipulators/collision-detection-and-control-of-parallel-structured-flexible-manipulators-based-on-unscented-kalm>

INTECH
open science | open minds

InTech Europe

University Campus STeP Ri
Slavka Krautzeka 83/A
51000 Rijeka, Croatia
Phone: +385 (51) 770 447
Fax: +385 (51) 686 166
www.intechopen.com

InTech China

Unit 405, Office Block, Hotel Equatorial Shanghai
No.65, Yan An Road (West), Shanghai, 200040, China
中国上海市延安西路65号上海国际贵都大饭店办公楼405单元
Phone: +86-21-62489820
Fax: +86-21-62489821

© 2010 The Author(s). Licensee IntechOpen. This chapter is distributed under the terms of the [Creative Commons Attribution-NonCommercial-ShareAlike-3.0 License](#), which permits use, distribution and reproduction for non-commercial purposes, provided the original is properly cited and derivative works building on this content are distributed under the same license.

IntechOpen

IntechOpen